The EMBO Journal (2008) 27, 2259–2269 | © 2008 European Molecular Biology Organization | Some Rights Reserved 0261-4189/08
www.embojournal.org

THE EMBO JOURNAL

EMBO open

Structural basis for inhibition of homologous recombination by the RecX protein

Stefania Ragone[1], Joseph D Maman[1], Nicholas Furnham and Luca Pellegrini*

Department of Biochemistry, University of Cambridge, Cambridge, UK

The RecA/RAD51 nucleoprotein filament is central to the reaction of homologous recombination (HR). Filament activity must be tightly regulated *in vivo* as unrestrained HR can cause genomic instability. Our mechanistic understanding of HR is restricted by lack of structural information about the regulatory proteins that control filament activity. Here, we describe a structural and functional analysis of the HR inhibitor protein RecX and its mode of interaction with the RecA filament. RecX is a modular protein assembled of repeated three-helix motifs. The relative arrangement of the repeats generates an elongated and curved shape that is well suited for binding within the helical groove of the RecA filament. Structure-based mutagenesis confirms that conserved basic residues on the concave side of RecX are important for repression of RecA activity. Analysis of RecA filament dynamics in the presence of RecX shows that RecX actively promotes filament disassembly. Collectively, our data support a model in which RecX binding to the helical groove of the filament causes local dissociation of RecA protomers, leading to filament destabilisation and HR inhibition.

The EMBO Journal (2008) **27,** 2259–2269. doi:10.1038/emboj.2008.145; Published online 24 July 2008
Subject Categories: genome stability & dynamics; structural biology
Keywords: genomic stability; homologous recombination; RecA; RecX

Introduction

Homologous recombination (HR) is necessary for the accurate repair of double-strand (ds) breaks in the DNA and is crucial for maintaining genome integrity (van Gent *et al*, 2001; West, 2003). The conserved RecA-like DNA strand-exchange proteins are DNA-dependent ATPases that polymerise on single-stranded DNA (ssDNA) to form a right-handed nucleoprotein filament, the molecular species that performs the homologous pairing and strand-exchange reactions of HR (Brendel *et al*, 1997; Roca and Cox, 1997; Bianco *et al*, 1998; Lusetti and Cox, 2002; Schlacher *et al*, 2006; Cox, 2007a, b). Uncontrolled recombination can lead to genomic instability and as a result the activity of the nucleoprotein filament is finely tuned by a range of regulatory mechanisms that can promote or repress HR (Sung and Klein, 2006). In bacteria, RecA activity is modulated by a growing network of functional interactions that are only partially understood (Cox, 2007b). The single-strand-binding (SSB) protein coats exposed ssDNA, removing DNA secondary structure in the process and inhibiting binding of RecA (Kowalczykowski and Krupp, 1987; Lavery and Kowalczykowski, 1990; Hobbs *et al*, 2007). The RecBCD complex degrades the ends of a dsDNA break and loads RecA on the resulting 3′-end ssDNA tail in preparation for strand exchange (Kowalczykowski, 2000). The RecR, RecO and RecF proteins cooperate to promote RecA filament assembly on gapped DNA coated with SSB, possibly limiting filament extension onto dsDNA (Umezu *et al*, 1993; Umezu and Kolodner, 1994; Shan *et al*, 1997; Webb *et al*, 1997; Bork *et al*, 2001b; Morimatsu and Kowalczykowski, 2003). RecF is also capable of promoting RecA filament activity by counteracting the effect of the negative regulator RecX (Lusetti *et al*, 2006). The DinI protein stabilises RecA filaments (Lusetti *et al*, 2004), whereas the role of PsiB and RdgC in RecA filament activity is still unclear (Bailone *et al*, 1988; Moore *et al*, 2003). The UvrD helicase can disassemble RecA filaments *in vitro* and may be involved in destabilising recombination intermediates (Mendonca *et al*, 1993; Morel *et al*, 1993; Veaute *et al*, 2005).

The *Escherichia coli recX* gene is located immediately downstream of the *recA* gene. Both genes are expressed from the same cistron, which is under the transcriptional control of the LexA repressor (Pages *et al*, 2003). In *E. coli*, a DNA hairpin between the *recA* and *recX* genes allows 5–10% transcriptional read-through of the *recX* gene, resulting in lower levels of the RecX protein relative to RecA (Pages *et al*, 2003). The RecX protein is required to overcome the effect of overexpressing RecA, suggesting that RecX is a negative regulator of RecA (Sano, 1993; Papavinasasundaram *et al*, 1997; Vierling *et al*, 2000; Sukchawalit *et al*, 2001). Deletion of the *recX* gene did not result in a clear phenotype in *E. coli*, but overexpression of the *recX* gene inhibited induction of the SOS response (Pages *et al*, 2003; Stohl *et al*, 2003). *In vitro*, the RecX proteins from *Mycobacterium tuberculosis* and *E. coli* inhibited RecA-mediated strand exchange and ATPase activity, as well as co-protease function, at substoichiometric concentration relative to RecA (Venkatesh *et al*, 2002; Stohl *et al*, 2003; Drees *et al*, 2004b). Taken together, the evidence indicates that RecX represses HR by interfering with RecA functionalities.

The mechanism by which RecX regulates recombination is still unclear. Electron microscopy (EM) reconstructions of

*Corresponding author. Department of Biochemistry, University of Cambridge, 80 Tennis Court Road, Cambridge CB2 1GA, UK.
Tel.: +44 122 376 0469; Fax: +44 122 376 6002;
E-mail: lp212@cam.ac.uk
[1]These authors contributed equally to this work

Received: 25 January 2008; accepted: 1 July 2008; published online: 24 July 2008

AMP·PNP-stabilised RecA filaments on dsDNA in the presence of nearly stoichiometric concentration of RecX revealed that RecX can bind within the helical groove of the RecA nucleoprotein filament (VanLoock *et al*, 2003). As a result, it was suggested that repression of recombination might occur by steric clash of RecX with the strand-exchange reaction, as well as by prevention of the ATP-coupled allosteric changes in RecA that are required for recombination (VanLoock *et al*, 2003). An alternative model for RecX-dependent inhibition of recombination was based on its proposed ability to cap the growing 3′-end of the RecA filament, resulting in net disassembly of RecA protomers and eventual dissolution of the filament (Drees *et al*, 2004a).

In this paper, we describe a structural and functional analysis of the *E. coli* RecX protein and its interaction with the RecA nucleoprotein filament. The crystal structure of RecX reveals a modular architecture of tandem helical repeats, which is strongly suggestive of a mechanism of interaction with the RecA filament. We define a conserved, positively charged surface of RecX as important for its inhibitory function and test this assumption by defining RecX mutants with weakened ability to repress RecA function *in vitro*. The structural and biochemical data are complemented by a functional analysis that demonstrates how RecX actively promotes RecA dissociation from established filaments. We integrate our findings and existing data in a model of RecX function, which provides a novel example of the variety of mechanisms that regulate HR by interference with the activity of the nucleoprotein filament.

Results

Modular architecture of the RecX structure

Initial crystallisation trials with wild-type RecX were unsuccessful. Mutation of cysteine residues 113 and 118 to alanine generated a version of the RecX protein that yielded crystals suitable for high-resolution X-ray analysis. The crystal structure was solved to a resolution of 1.8 Å using the anomalous signal of selenomethionine-derivatised protein (Supplementary Table 1). In the crystals, two RecX chains related by a non-crystallographic two-fold axis share an unusually large interface that buries 2800 $Å^2$ of solvent-accessible surface. The homodimeric form of RecX appears to be an artefact of crystallisation because we could not detect it in solution using size-exclusion chromatography, homo-bifunctional chemical crosslinking (not shown), or sedimentation velocity in an analytical ultracentrifuge (Supplementary Figure 1). The mutagenesis required to induce crystallisation did not impair RecX function (Supplementary Figure 2).

The crystallographic analysis demonstrates that RecX is a modular protein, consisting of three copies of a three-helix bundle of approximately 50 amino acids each that assemble in tandem repeats, resulting in an elongated protein shape of approximate overall dimensions of 70 Å × 20 Å × 20 Å (Figure 1). The relative arrangement of the three repeats imparts a moderate degree of curvature to the long axis of the RecX structure, resulting in a somewhat flat concave surface on one side and a convex surface on the other side of the molecule. Despite the low degree of sequence similarity, the three repeats can be superimposed with an overall r.m.s.d. of 1.7 Å over 37 aligned C_α positions (Figure 1B). Although the modular nature of the RecX structure could not be detected by inspection of the amino-acid sequence, structural superposition of the three repeats identifies several residues that are preferentially occupied by hydrophobic amino acids (Figure 1D). The most likely explanation for their conservation is their important structural role in RecX folding. Amino acids 113 and 118, which were mutated from cysteine to alanine to induce crystallisation, occupy solvent-exposed positions on the convex side of the protein.

Structural comparison of the RecX structure against the Protein Data Bank (PDB) archive in SSM (http://www.ebi.ac.uk/msd-srv/ssm/) did not find any reliable match, suggesting that the RecX fold is unique. However, the structure of the isolated RecX repeat represents a convincing 3D match for helix-turn-helix (HTH) DNA-binding domains found in homeodomain transcription factors and site-specific recombination enzymes: RecX repeat 2 can be superimposed to the Oct-1 POU homeodomain of PDB entry 1POG with an r.m.s.d. of 1.9 Å over 41 C_α positions (Figure 1C). A weaker structural similarity can also be detected between a RecX segment spanning repeats 1 and 2 and the two HTH modules of the MarA transcriptional activator (PDB entry 1BL0). Thus, RecX extends our knowledge of tandem repeat proteins as a remarkable example of protein architecture assembled by consecutive copies of an HTH-like domain. The finding that the RecX repeats resemble DNA-binding domains raises the possibility that RecX might bind DNA. Published evidence shows that RecX can bind both ss- and dsDNA, but the functional relevance of these observations is still unclear (Stohl *et al*, 2003; Drees *et al*, 2004a; Galvao *et al*, 2004).

Inspection of the RecX structure reveals the presence of considerable repeat–repeat interfaces: inter-repeat contacts bury 779 $Å^2$ and 965 $Å^2$ of accessible surface area at the 1–2 and 2–3 repeat interfaces, respectively. The tight packing of the repeats fixes their relative orientation and confers overall rigidity to the structure. Notable common features of the repeat–repeat interface include the presence of a conserved glycine residue in the tight connection between helices II and III of repeats 2 and 3 (G100 and G151, respectively), which allows for close head-to-tail packing of helix II in the three repeats (Supplementary Figure 3). The interface between repeats 2 and 3 is particularly extensive: W117 at the N terminus of helix I in repeat 3 links the interior of repeats 2 and 3 in an hydrophobic continuum (Supplementary Figure 3). The smaller hydrophobic component of the interface between repeats 1 and 2 is compensated for by additional polar interactions: particularly prominent are the partially buried, bidentate interactions linking the carboxylate of D71 at the N terminus of helix I in repeat 2 to the main chain nitrogen atoms of E29 and Q30 in repeat 1; and the carbonyl moiety and Nζ nitrogen atom of K99 at the C terminus of helix II in repeat 2 with the side chains of S28 and E31, respectively, in helix II of repeat 1 (Supplementary Figure 3).

Surface properties of the RecX structure

The available evidence indicates that RecX regulates HR by direct interaction with the RecA nucleoprotein filament (VanLoock *et al*, 2003; Drees *et al*, 2004a). To gain an insight about the structural epitopes of the molecule that might be responsible for protein–protein and protein–DNA interactions, we analysed the charge distribution of the RecX surface. The outstanding feature of the electrostatic properties of RecX is the opposite polarity of the charge distribution on its

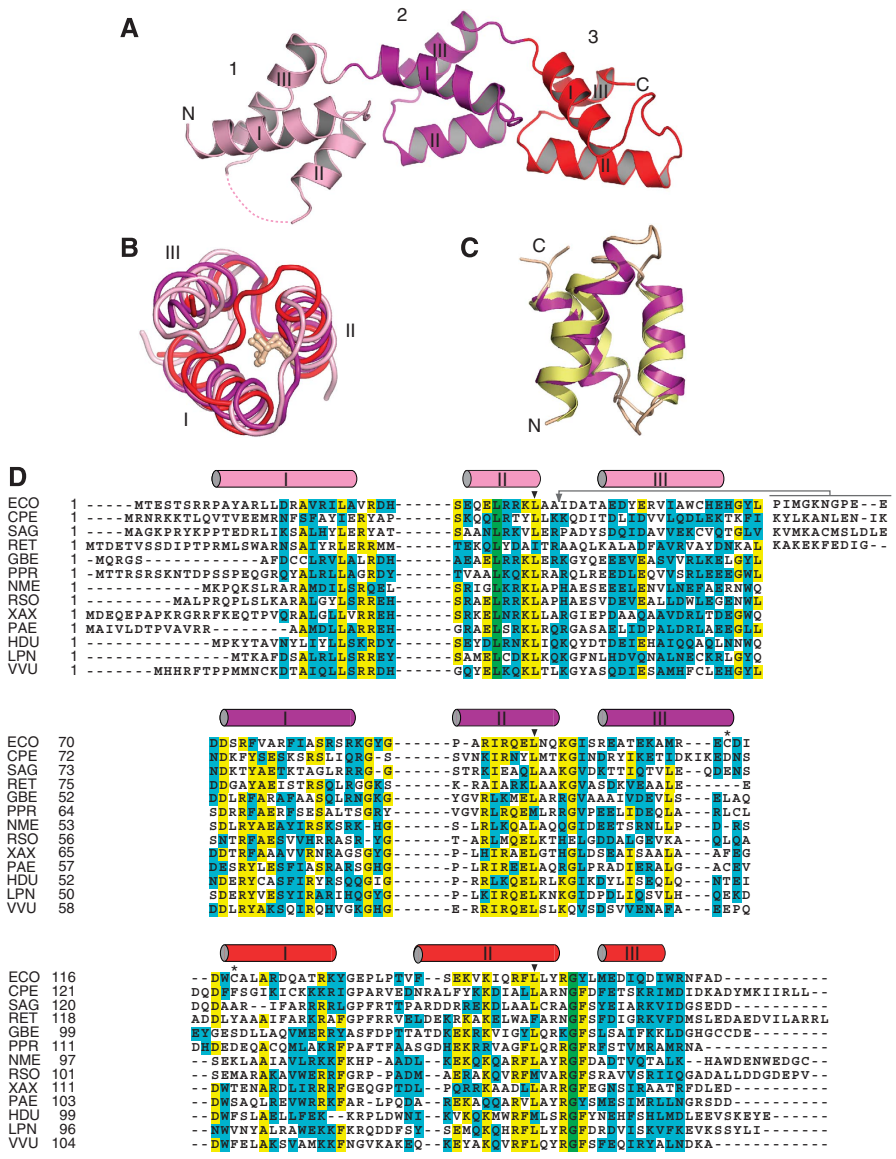

Figure 1 3D structure of the RecX protein. (**A**) The RecX structure consists of three tandem repeats of a three-helix motif. The cartoon representation of RecX highlights the modular nature of its structure. The three repeats are coloured pink (1), purple (2) and red (3), from the N- to the C-terminal end of the protein. The helices of the three-helix motif are numbered in roman numerals. (**B**) Structural superposition of the three repeats of RecX. Colour coding is as in (A). The side chain of a highly conserved hydrophobic residue in helix II of the three repeats (L36, L96 and L147) is shown in ball-and-stick representation; its position in the multiple sequence alignment of (D) is marked with a black triangle. (**C**) Structural superposition of repeat 2 of RecX (purple) with the homeodomain of the Oct-1 Pou protein (PDB entry 1POG), in yellow. (**D**) Structure-based multiple sequence alignment of proteobacterial RecX sequences (ECO, *Escherichia coli*; CPE, *Candidatus pelagibacter*; SAG, *Stappia aggregata*; RET, *Rhizobium etli*; GBE, *Geobacter bemidjiensis*; PPR, *Pelobacter propionicus*; NME, *Neisseria meningitidis*; RSO, *Ralstonia solanacearum*; XAX, *Xanthomonas axonopodis*; PAE, *Pseudomonas aeruginosa*; HDU, *Haemophilus ducreyi*; LPN, *Legionella pneumophila*; VVU, *Vibrio vulnificus*). Similar residues are in cyan, identical residues in yellow and completely conserved residues in green. The position of the three alpha-helices for each of the three repeats is marked above the alignment; the helices are coloured as in (A). The alignment is split into three parts according to repeat boundaries. The sequences of the repeats are arranged so that structurally equivalent residues are vertically aligned over the three repeats. A sequence insertion in the alignment of the N-terminal repeat is shown to the right side of the alignment. The position of C113 and C118 that were mutated to alanine for RecX crystallisation is indicated by an asterisk.

concave and convex sides: the concave face of RecX is almost uniformly positively charged, whereas the convex face is predominantly negative (Figure 2A). Thus, the electrostatic analysis of the RecX surface indicates that RecX is a highly polarised molecule and suggests that the peculiar charge distribution of the protein might have an important role in its function.

Solvent-exposed regions of a protein that are involved in functional interactions with other macromolecules are subject to stronger evolutionary pressure and therefore show a higher degree of amino-acid conservation than otherwise expected for surface residues. We used the ConSurf server (http://consurf.tau.ac.il/) to map the extent of phylogenetic conservation of RecX residues on our crystallographic model (Landau *et al*, 2005). The structure-based phylogenetic analysis highlights another striking aspect of the RecX protein: the solvent-exposed amino acids on the concave face of the protein present a higher degree of

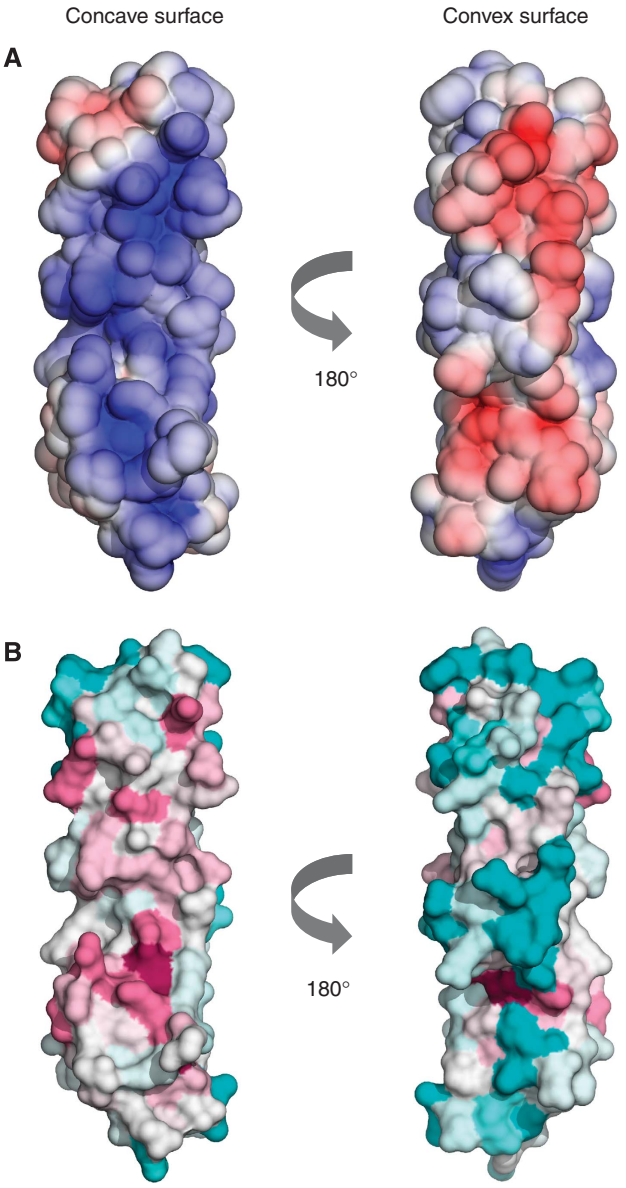

Figure 2 Surface properties of the RecX protein. The two views in (**A**, **B**) show the concave and convex surfaces of the protein, obtained by a 180° rotation on the long axis of the molecule. (A) Electrostatic properties of the RecX protein. The electrostatic potential was calculated with APBS (Baker *et al*, 2001) and mapped onto the solvent-accessible surface of the molecule, at contouring levels of ±5 kT (blue/red). The concave and convex sides of the protein display surface potentials of opposite charge. (B) Evolutionary conservation of surface residues in RecX, calculated with ConSurf (Landau *et al*, 2005) from a structure-based alignment of 74 RecX sequences. Amino-acid conservation on the molecular surface of the protein is indicated by a transition in colour hues, from magenta (most conserved) to cyan (most variable).

conservation relative to residues of the convex side (Figure 2B).

Inspection of the concave surface of RecX reveals the presence of an extensive network of side chain–side chain interactions involving basic and aromatic residues (Figure 3A). The program CaPTURE (Gallivan and Dougherty, 1999) identifies five of these contacts as energetically significant cation–π interactions: F78–R82, R82–Y87, Y87–R150, K128–F146 and R145–Y149. The mesh of cation–π contacts immobilise the side chains of conserved basic residues R82, K128, R145 and R150, thus keeping them poised for potential interaction. The potential for hydrophilic interaction of the concave surface is augmented by side chains of R25, K35, R91, K99, R127 and K142 that line the perimeter of the cation–π interaction network.

Structure-based mutational analysis of RecX function

Examination of the RecX structure suggested that its conserved, positively charged concave face might represent a functional surface. We therefore selected for mutagenesis the conserved lysine and arginine residues R25, K35, R127, K128, R145 and analysed the ability of the mutant proteins to inhibit RecA activity. The functional importance of the selected amino acids was tested by mutation to glutamic acid, which reverses the charge of the residue while preserving its hydrophilic nature. In the case of residues participating in cation–π contacts (K128 and R145), mutation was to methionine, to maintain the hydrophobic component of the interaction. The RecX mutants were tested for their ability to suppress the ATPase and strand-exchange activities of the RecA filament. The experiments were performed with a range of RecX concentrations to explore the variation in potency between the mutant and wild-type proteins.

All RecX mutants showed reduced inhibition of ATP hydrolysis by the RecA filament relative to wild-type RecX, albeit with considerable differences in their effectiveness (Figure 3B). Examination of the concentration dependency of RecA inhibition allowed ranking of the RecX mutants as: R25E > R145M > K128M ~ K35E > R127E, in order of decreasing efficacy. R25E was the most effective mutation, extinguishing RecX-dependent inhibition almost completely even at the highest concentration tested (0.8 μM; 1:2.5 ratio of RecX to RecA). The results of the strand-exchange inhibition experiments confirmed that R25E is the most effective single-point mutation in compromising RecX function, whereas the R145M mutant displayed only a mild impairment and the K35E, R127E, K128M mutants behaved similar to wild-type RecX (Figure 4). A double mutation of R25E and R127E showed the strongest effect on RecX-dependent inhibition, rendering the protein virtually inactive in both ATPase and strand-exchange assays at all tested concentrations.

These observations implicate conserved basic residues on the concave surface of RecX in the repression of RecA filament activity. The solvent-exposed R25 in the linker between helices I and II of repeat 1 appears to be particularly important for RecX function. However, the involvement of spatially distant residues in RecX's inhibitory function suggests that the integrity of all or most of the concave surface of RecX is required for optimal function.

Interaction of RecX with the RecA filament

The structure of RecA–dsDNA–AMP·PNP filaments in the presence of RecX, at a 1:1 stoichiometric ratio of RecX to RecA, was investigated by EM (VanLoock *et al*, 2003). The EM analysis detected additional density located deep inside the helical groove of the RecA filament, which was attributed to RecX. The selection for 3D reconstruction of filament segments enriched in RecX density and the helical averaging of the filament structure resulted in a continuous tubular density wound around the filament axis. Docking of the

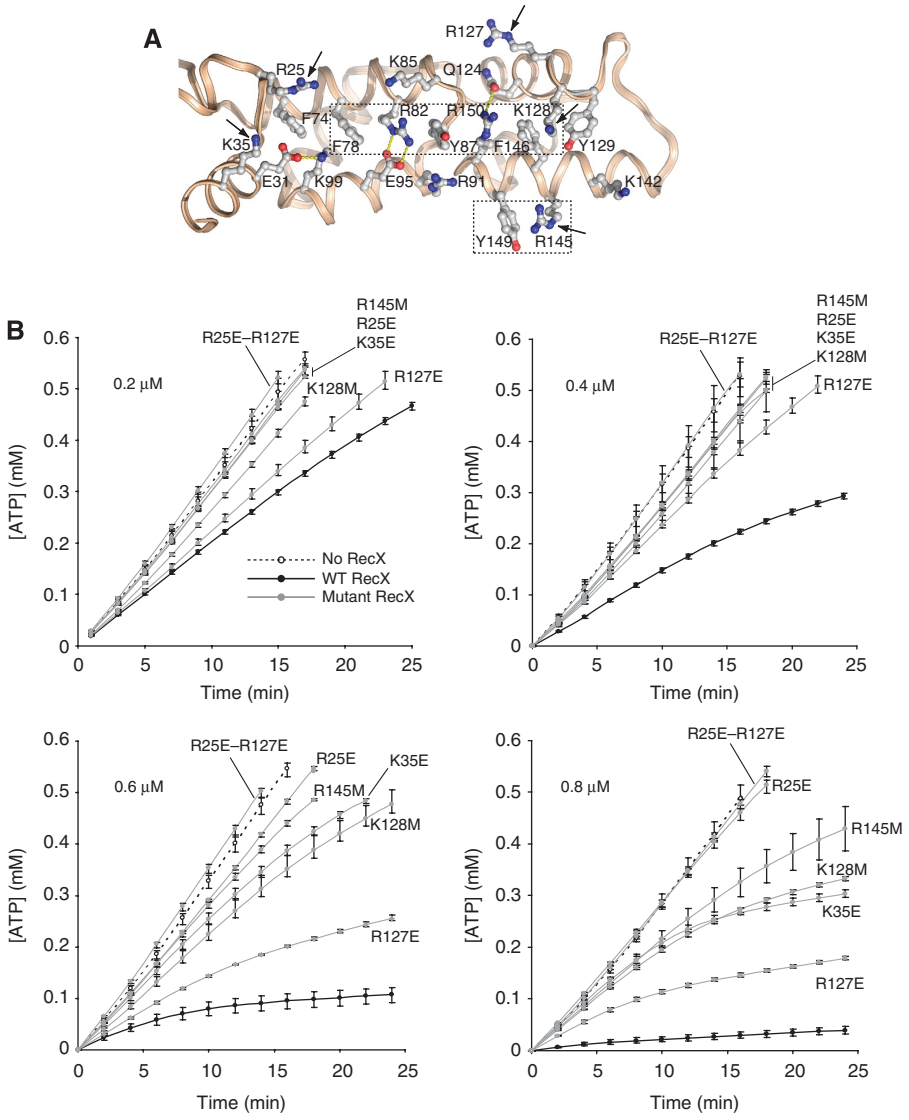

Figure 3 Structure-based mutational analysis of RecX. (**A**) Basic residues on the conserved concave face of RecX. Aromatic residues involved in cation–π interactions with basic side chains, as well as glutamic and glutamine residues hydrogen bonded to the basic side chains, are also shown. Cation–π interactions that are energetically significant according to the program CaPTURE (Gallivan and Dougherty, 1999) are enclosed within a dashed-line box. The RecX polypeptide is represented by a ribbon, whereas side chains are drawn in ball-and-stick representation. Basic residues selected for mutagenesis are indicated by arrows. (**B**) Inhibition of RecA's DNA-dependent ATPase activity by wild-type and mutant RecX proteins. Each graph shows the amount of ATP hydrolysed by RecA in the presence of the various RecX mutants (see Materials and methods for details). The assay was performed at four different RecX concentrations, reported in each graph. Each data point represents the average of three simultaneous measurements.

crystallographic model of RecX in the EM reconstruction reveals that the volume and shape of the protein fit well into the additional RecX-associated density (Figure 5).

Although it is impossible to fix the position of RecX in the continuous density of the reconstructed filament, it is clear that the curvature of the RecX structure appears well suited to match the helical groove of the filament. As a result of the docking, the conserved, functionally active concave surface of RecX faces inwards towards the filament axis, in a suitable position to interact with both DNA and RecA. We note that the strongly basic nature of the concave surface of RecX would complement the polyanionic nature of DNA and the overall negative charge of the RecA C terminus, which mediates in part the interaction with RecX (Drees *et al*, 2004b). Taken together, the functional analysis of RecX mutants and the docking of the RecX structure into the EM reconstruction of the RecA–RecX nucleoprotein filament suggest that RecX inhibits RecA functions by binding within the helical groove of the filament through its positively charged, concave surface.

RecX actively removes RecA from nucleoprotein filaments

After nucleation on ssDNA, RecA filaments grow by the net addition of RecA protomers to the 3′-end of the filament and shrink by net release of RecA protomers from the 5′-end; a higher rate of RecA binding at the 3′-end relative to the rate of RecA dissociation at the 5′-end results in increased filament size (Lindsley and Cox, 1990; Shan *et al*, 1997; Bork *et al*, 2001a; Galletto *et al*, 2006; Joo *et al*, 2006). Drees *et al* (2004a) suggested that RecX performs its inhibitory function by binding to the 3′-end of the RecA filament, in a manner

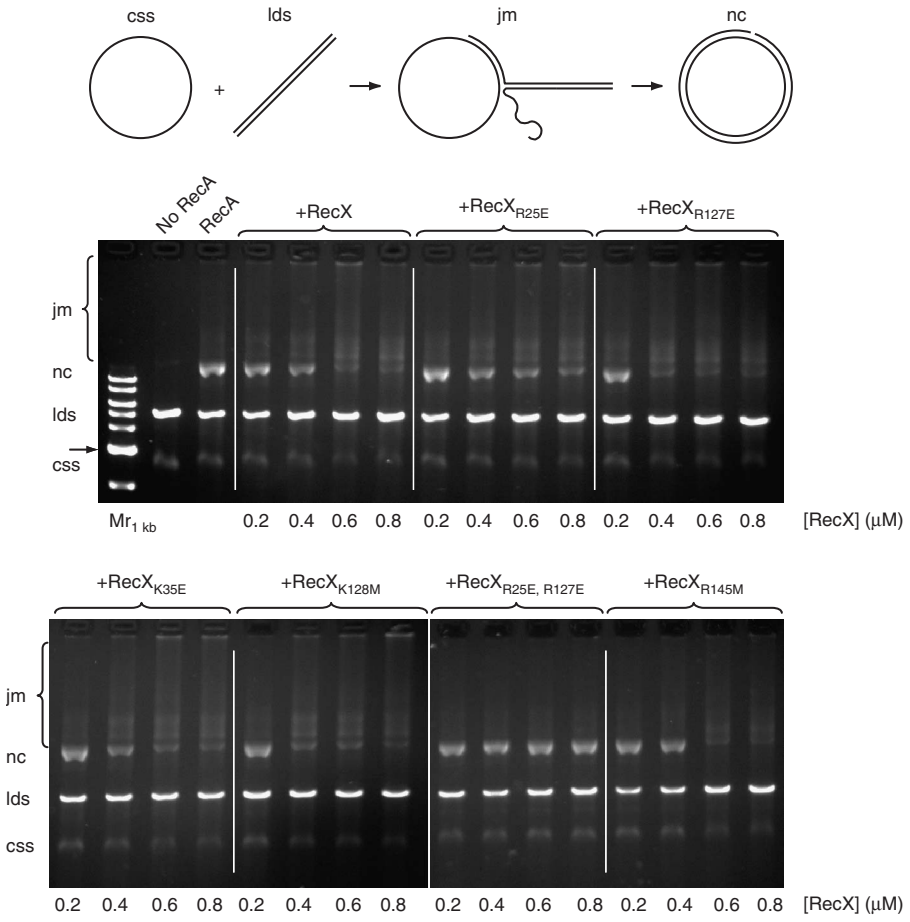

Figure 4 Inhibition of RecA's strand-exchange activity by wild-type and mutant RecX proteins. The strand-exchange reactions were incubated at 37°C for 45 min with the concentration of wild-type and mutant RecX indicated below each lane (see Materials and methods for details). css: circular single-stranded DNA; lds: linear double-stranded DNA; jm: joint molecule; nc: nicked circle (product of reaction). The position of the 3 kb band in the dsDNA 1 kb ladder (NEB) is indicated by an arrow for reference.

that prevents further addition of RecA protomers to the growing end of the filament. As filament disassembly continues unimpeded from the 5′-end, 'capping' of the 3′-end by RecX would lead over time to filament dissolution.

We chose to test current models of RecX function by surface plasmon resonance (SPR). Nucleoprotein filaments were generated by binding RecA to a 5′-biotinylated ssDNA (60-mer oligo-dT) immobilised on a streptavidin (SA)-coated sensor chip (Figure 6A). RecA was injected into the flow cells until the binding curve indicated that maximal saturation had been achieved. We confirmed that the dynamic behaviour of RecA filaments reconstituted on the SA chip was as previously reported by examining the dependency of RecA dissociation on ATP hydrolysis (Lindsley and Cox, 1990; Arenson *et al*, 1999; Galletto *et al*, 2006; Joo *et al*, 2006) (Supplementary Figure 4). The RecA filaments were then challenged by flowing RecX over the sensor chip. The set-up of the SPR experiment was designed so that it would be possible to discriminate between 'passive' and 'active' mechanisms of RecX action. In fact, no RecA binding can take place after the initial injection, while dissociating RecA molecules are removed by the continuous flow in the system. Therefore, capping of the RecA filament at its 3′-end by the injected RecX would not alter the rate of RecA dissociation from the filament. Alternatively, any RecX-dependent mechanism involving active RecA removal from an established filament would alter the kinetic profile of filament disassembly.

The SPR analysis shows that RecX increases the rate of RecA dissociation from the filaments in a concentration-dependent manner (Figure 6B). The two RecX mutants, R25E–R127E and R145M, are impaired in their abilities to increase the rate of RecA filament disassembly compared with wild-type RecX (Figure 6C), a result that mirrors the effect of these mutants on RecA-dependent ATP hydrolysis. To test whether the effect of RecX depends on the ability of RecA to hydrolyse ATP, we reconstituted RecA filaments in the presence of the non-hydrolysable ATP analogue AMP · PNP. AMP · PNP increases considerably the rate of RecA binding to ssDNA, while causing a decrease in the rate of filament disassembly (Figure 6D). These observations agree with the augmented stability reported for RecA filaments formed in the presence of AMP · PNP (VanLoock *et al*, 2003) or ATPγS (Chabbert *et al*, 1987; Arenson *et al*, 1999; Galletto *et al*, 2006; Joo *et al*, 2006; Cisse *et al*, 2007). RecX increases the rate of RecA dissociation in a concentration-dependent manner, as observed for ATP. However, the effect of RecX on RecA dissociation is less pronounced in the absence of RecA-dependent ATP hydrolysis (Figure 6D).

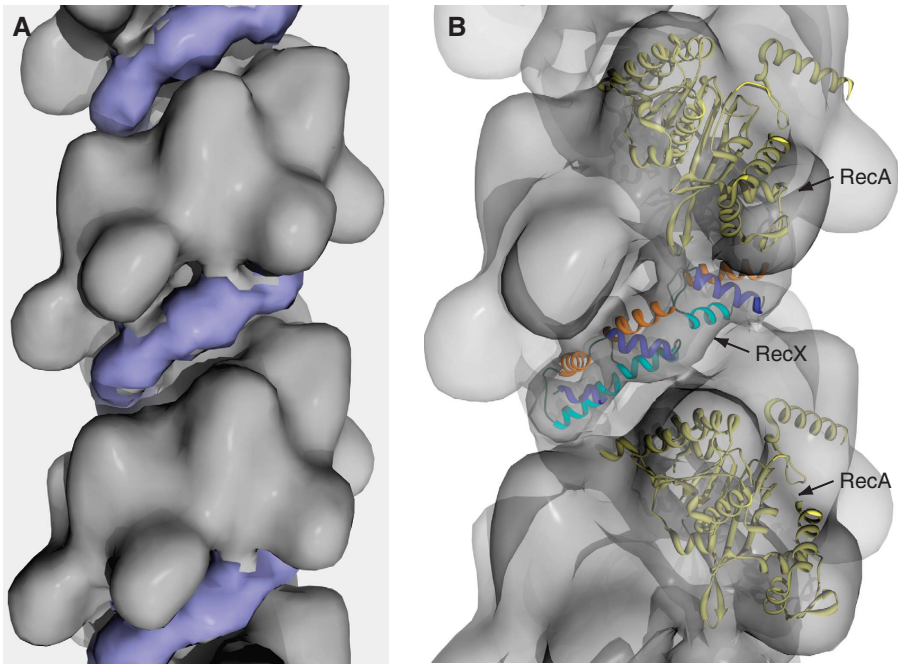

Figure 5 Interaction of RecX with the RecA nucleoprotein filament. (**A**) Solid surface representation of the EM reconstruction of a RecA–RecX–dsDNA–AMP · PNP filament. The extra-filament density ascribed to RecX is coloured in light blue, whereas the rest of the filament is coloured in grey. (**B**) The figure shows the proposed mode of interaction of RecX with the RecA filament, based on manual docking of the atomic model of RecX in the RecA–RecX–dsDNA–AMP · PNP filament. α-Helices in RecX are drawn as ribbons, coloured orange (helix I), cyan (helix II) and light blue (helix III) in all repeats. Two RecA protomers drawn as yellow ribbons have also been fitted in successive filament rungs, above and below RecX.

Discussion

In this paper, we have investigated the structural basis for the role of the RecX protein in HR. The crystal structure of RecX reveals an unanticipated modular architecture of three tandem repeats of a three-helix domain, bearing a clear resemblance to well-known DNA-binding HTH domains similar to the homeodomain. Thus, the crystallographic analysis of RecX increases our knowledge of the predominantly eukaryotic HTH domain by demonstrating its deployment in a novel structural and functional context. Furthermore, using a sequence profile derived from the structural superposition of the three repeats of *E. coli* RecX, it is possible to identify two additional repeats in the N- and C-terminal tails of a subset of RecX sequences that exceed the consensus size by about 100 amino acids (data not shown). The existence of polypeptides spanning five repeats confirms the modular nature of the RecX protein.

We identify the concave, positively charged face of the extended, curved protein shape as functionally important: mutations of conserved basic residues on the concave surface reduce the ability of RecX to inhibit RecA's ATPase and strand-exchange activities and to induce RecA filament depolymerisation. The phylogenetic and biochemical analyses indicate that the functionally relevant portion of the RecX surface is rather extensive, suggesting an intimate association of RecX with the protein and nucleic acid components of the RecA filament. Several conserved basic residues on the concave surface of RecX participate in an extended network of cation–π interactions, which constrain the basic side chains in a way that makes them poised for interaction. Involvement of functionally important side chains in a mesh of cation–π interactions might reduce the entropic cost associated with formation of a intermolecular interface and might also confer additional overall rigidity to the RecX structure.

By combining the crystal structure of RecX with the EM reconstruction of RecA–RecX filaments, it is possible to infer the mode of RecX interaction with the filament. EM analysis of RecA–dsDNA filaments stabilised by the ATP analogue AMP · PNP and in the presence of functional excess of RecX revealed additional density in the helical groove of the filament. Docking of the crystallographic model of RecX into the EM reconstruction showed a good agreement between the curved, elongated shape of the protein and the additional, tubular density present deep in the groove of the filament. Taken together, the structural and biochemical data indicate that RecX associates with the filament by arranging its elongated shape along the bottom of the continuous filament groove, with its positively charged concave side facing towards the axis of the filament, poised to interact with both protein and DNA. When bound to the filament, the elongated shape of RecX would permit contact with up to three consecutive RecA protomers, and could conceivably bridge RecA molecules on successive rungs of the filaments.

The structural evidence presented here does not support a mode of RecX binding that involves the specific recognition of the extremities of the RecA filament. In addition, the SPR analysis of the effect of RecX on the dynamic behaviour of RecA filaments shows that RecX actively promotes the dissociation of RecA from the filament. Accordingly, a satisfactory model of RecX's role in HR should account for its ability to bind anywhere along the filament and for its active role in promoting filament disassembly. Clearly, current mechanistic proposals of RecX function (VanLoock *et al*, 2003; Drees *et al*, 2004a) need to be integrated in a new model that can explain all the evidence now available. Thermodynamic considerations

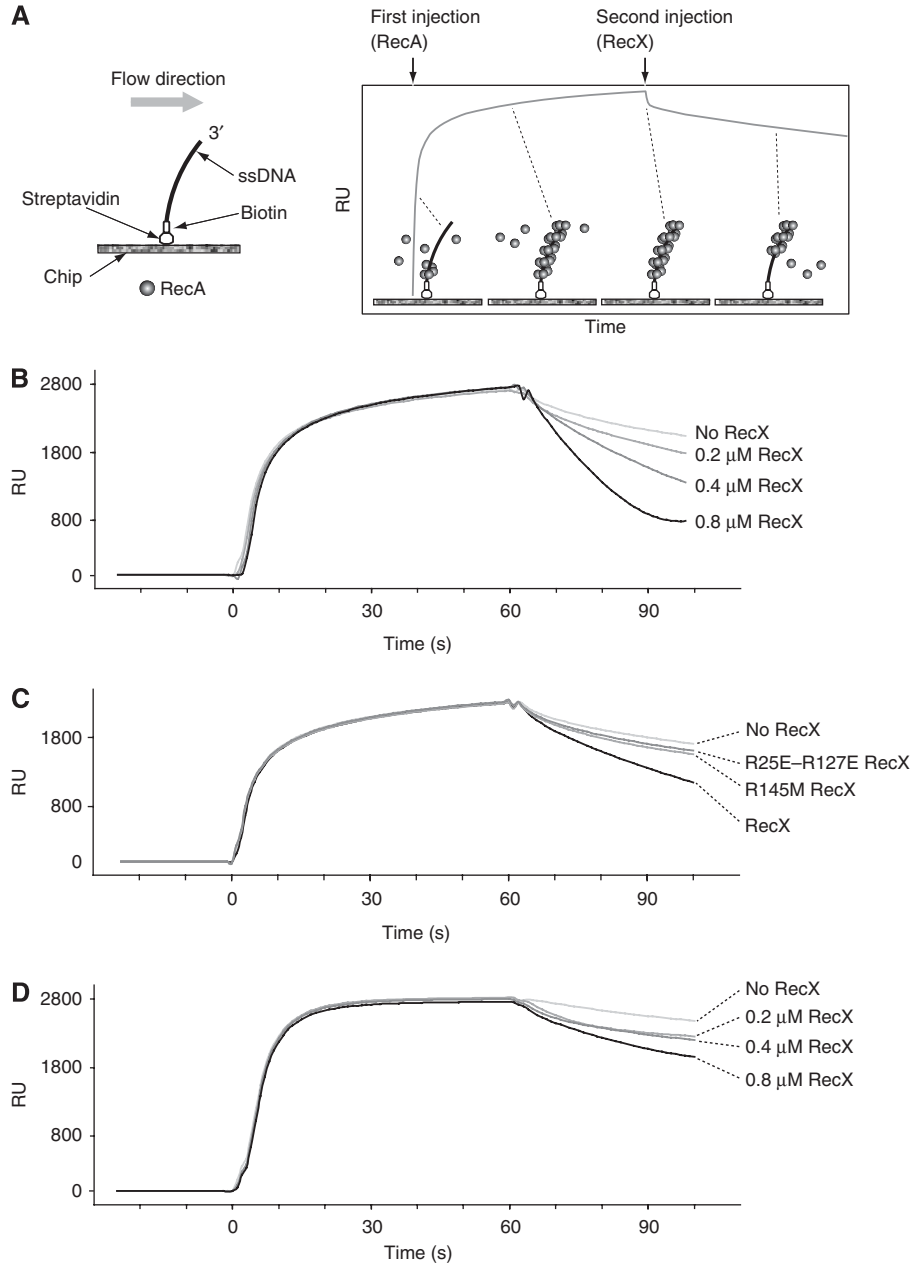

Figure 6 RecX increases the rate of RecA filament disassembly. (**A**) Illustrative diagram of the surface plasmon resonance experiment, detailing the linkage of the ssDNA substrate to the sensor chip, and the various stages of RecA filament assembly and dissociation during the experiment. RU is resonance units. (**B**) The effect of RecX concentration (reported in the panel) on the dissociation rate of RecA filaments. (**C**) The effect of wild-type and mutant R145M, R25E-R127E RecX proteins on the dissociation rate of RecA filaments. RecX concentration in the experiment was 0.4 μM for wild-type and mutant proteins. (**D**) Same as in (B), except that the non-hydrolysable analogue AMP · PNP was used instead of ATP.

predict that filament disassembly does not ensue by dissociation of RecA protomers from internal sites of the filament (McGhee and Von Hippel, 1974; Schwarz and Watanabe, 1983). Indeed, single-molecule fluorescence assays demonstrated that RecA protomers dissociate preferentially from filament ends (Joo *et al*, 2006). Thus, to promote filament disassembly RecX must either enhance the rate of RecA dissociation per filament end or increase the actual number of ends. We favour the latter proposition as it accounts for RecX's ability to bind anywhere along the filament. We propose that binding of RecX within the helical groove of the nucleoprotein filament might facilitate the removal of one or more RecA protomers, thus generating a discontinuity in the RecA coating of the DNA. Dissociation of RecA would then commence from the newly generated 5′-end, whereas the continuing association of RecX near the newly created 3′-end would prevent further addition of RecA protomers. Thus, the extent of RecA dissociation would be proportional to RecX concentration: the more RecX molecules bind to the filament, the more filament interruptions would occur, therefore increasing the overall rate of filament disassembly (Figure 7).

Our understanding of the molecular mechanisms by which nucleoprotein filament activity is regulated during HR is still limited. We were initially motivated to investigate the molecular basis of RecX function by the realisation of functional

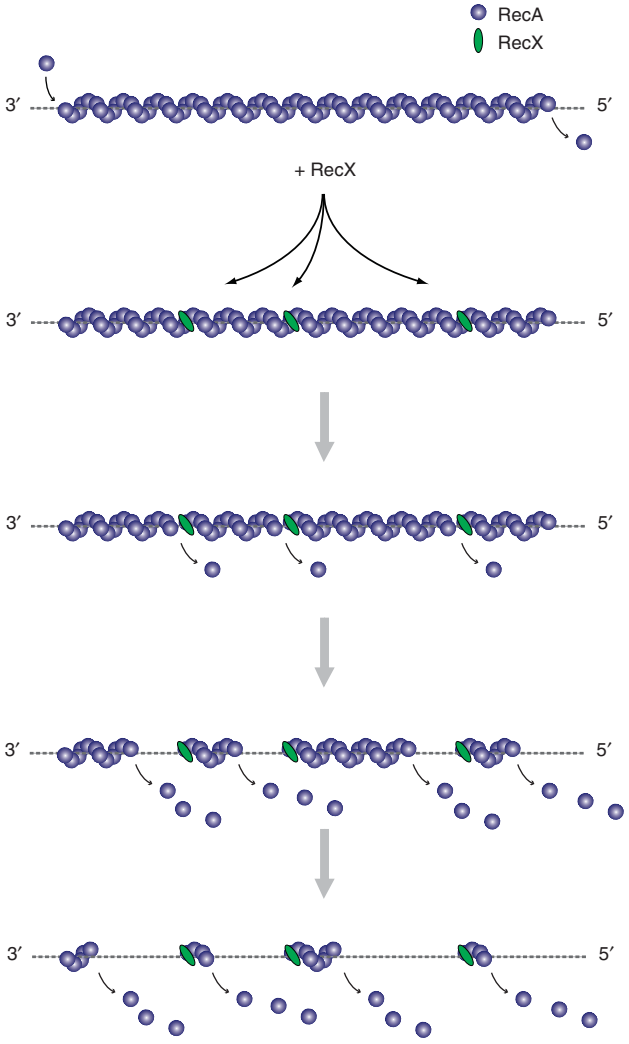

Figure 7 Model of RecX-dependent destabilisation of RecA nucleoprotein filaments. RecX binding to the filament causes localised dissociation of RecA protomers and increased number of 5′-ends, leading to overall filament disassembly.

similarities in the ability of RecX and the BRC repeat sequences of the breast cancer susceptibility protein BRCA2 to disassemble nucleoprotein filaments. This study has uncovered a structurally novel mechanism of HR regulation, based on a modular protein architecture that has evolved to interact directly within the groove of the nucleoprotein filament. The novelty of our findings hints at a fascinating range of regulatory mechanisms that awaits structural and biochemical characterisation.

The crystal structure of pre- and postsynaptic RecA–DNA complexes was reported while our paper was under revision (Chen *et al*, 2008). These crystallographic models allow for the first time the visualisation of ss- and dsDNA within the RecA nucleoprotein filament. Molecular docking of the RecA–dsDNA complex (PDB entry 3CMX) in the EM reconstruction of the RecA–RecX–dsDNA filament confirms that RecX can interact with both protein and nucleic acid components of the filament through its concave surface. Furthermore, the docking analysis shows that filament-bound RecX would be well positioned to make extensive contacts with the phosphate backbone of the postsynaptic strand of DNA.

Materials and methods

Cloning, mutagenesis, expression and purification of proteins

The *recX* gene was amplified from *E. coli* genomic DNA and a nucleotide sequence coding for amino acids 9–166 of the RecX protein was cloned into the 'Gateway' (Invitrogen) expression system following the manufacturer's protocol. The upstream oligo contained an in-frame PreScission protease cleavage site between the Att site and the *recX*-coding sequence. The destination expression vector (pETG-10A, EMBL Heidelberg) contained an in-frame hexa-histidine tag upstream of the 5′ Att site. The cells were grown in Turbo Broth™ Media (Athena Enzyme System), 100 μg/ml ampicillin, at 37°C and 250 r.p.m. RecX expression was induced with 1 mM, isopropyl-β-D-thiogalactopyranoside at $OD_{600} = 0.5$ and the incubation was continued for 3 h. The cells were harvested by centrifugation, resuspended in 20 mM Tris–HCl pH 8.0, 500 mM NaCl (buffer A), containing protease inhibitors cocktail (Complete EDTA-free; Roche) and lysed by sonication. The insoluble cellular material was removed by centrifugation at 40 000 *g* for 30 min, at 4°C. All the following steps were carried out at room temperature. The clarified lysate was loaded at 1 ml/min on a His-Select-Cartridge (Sigma) equilibrated in buffer A. The cartridge was washed with buffer B (buffer A plus 30 mM imidazole) and RecX was eluted with buffer C (buffer A plus 200 mM imidazole) followed by buffer D (buffer A plus 400 mM imidazole). Fractions containing RecX were pooled, and the histidine tag was cleaved by overnight dialysis against buffer A in the presence of 200 U of PreScission protease (GE Healthcare) and 1 mM DTT. The dialysed digest was centrifuged to remove precipitate, diluted with 20 mM Tris–HCl pH 8.0 to 350 mM NaCl, and filtered. The diluted digest was loaded on a anion-exchange ResQ column equilibrated with 20 mM Tris–HCl, 350 mM NaCl, 1 mM DTT, and RecX was collected in the flow-through. The protein was concentrated (Amicon Ultra 15; MWCO 10 000) to a volume of 3–5 ml, loaded on a Superdex 200 16/60 column (GE Healthcare) equilibrated with buffer A containing 1 mM DTT (biochemical experiments) or 20 mM Tris–HCl, 0.2 M arginine, pH 8.0 (crystallography). Mutant RecX proteins were purified in the same way. Selenomethionine-derivatised RecX was expressed in B834(DE3)-competent cells (Novagen) and purified in the same way. RecX mutants were generated using the QuickChange® II Site-Directed Mutagenesis Kit (Stratagene).

E. coli RecA was expressed in Tuner (DE3) cells (Novagen) by transformation with pTXB-recA3. The cells were grown in M9Y media (Athena Enzyme System), with 200 μg/ml ampicillin. The harvested cells were lysed by sonication in a buffer containing 25% sucrose w/v, 80 mM Tris–HCl pH 7.5, 5 mM EDTA, protease inhibitor cocktail (Complete, EDTA-free; Roche), and 12 500 U/1 l culture of Benzonase (Novagen). The rest of the purification procedure was as described (Singleton *et al*, 2002).

Crystallisation and X-ray structure determination

RecX was crystallised by hanging-drop vapour diffusion at 18 °C against a crystallisation buffer containing 0.1 M Tris–HCl pH 8.5, 0.2 M sodium acetate, 15% PEG4000, at 3–5 mg/ml protein concentration. Crystallisation required site-directed mutagenesis that replaced cysteines 113 and 118 with alanine. Initial crystalline material was improved by streak seeding techniques. The crystals belong to orthorombic space group $P2_12_12_1$ with cell dimensions: $a = 55.5$, $b = 71.8$ and $c = 74.7$ Å and two protein molecules in the asymmetric unit. The diffraction data were collected at beamline ID29 of the ESRF (Grenoble, France). The X-ray structure was solved with phase information obtained from multiple anomalous scattering experiments on selenomethionine-containing crystals. The position of the selenium atoms was determined by Shake-and-Bake (Weeks and Miller, 1999) and an initial solvent-modified map was calculated in SHARP (La Fortelle and Bricogne, 1997). A complete crystallographic model of RecX was obtained iteratively through the use of RAPPER (Furnham *et al*, 2006), Phenix (McCoy *et al*, 2007) and ArpWarp (Morris *et al*, 2003) together with some manual model building. The final crystallographic model was refined with REFMAC5 (Murshudov *et al*, 1997) and COOT (Emsley and Cowtan, 2004), to R and R_{free} values of 0.182 and 0.223 respectively, at a resolution of 1.8 Å. Amino acids 40–50 of chain A and the five C-terminal residues of both chains are disordered in the electron density and are therefore not included in the final model. The conformation of amino acids 40–50 of chain B

must be considered tentative as the electron density in this region of the map is poor. Extra density at the N terminus of both RecX chains has been modelled as a glycine residue of the recognition sequence of the PreScission protease. The refined crystallographic model of RecX contains 264 residues (98.88%) in the preferred region of the Ramachandran plot, two residues in the allowed region and one outlier. Coordinates and structure factors have been deposited in the PDB with accession code 3C1D. Figures were generated with PyMOL (http://pymol.sourceforge.net) and Chimera (http://www.cgl.ucsf.edu/chimera).

ATPase assay

RecA enzyme-linked ATPase assays were performed essentially as described (Drees *et al*, 2004a) adapted for a microplate-based photometric assay as described (Kiianitsa *et al*, 2003). All incubations were at 37°C. ϕX174 circular ssDNA at a concentration of 15 μM (nucleotide concentration) (New England Biolabs) was incubated for 5 min in a buffer containing 25 mM Tris–acetate pH 7.5, 10 mM Mg-acetate, 3 mM K-glutamate (SE buffer) and in the presence of 1 mM DTT, 0.1 mg/ml BSA (New England Biolabs), an ATP-regenerating system consisting of 3 mM phosphoenolpyruvate (PEP) and pyruvate kinase–lactate dehydrogenase mix (22.8 and 17.6 U/ml, respectively; Sigma), 1.5 mM NADH, 5 mM ATP and 0.64 μM SSB protein (Sigma). ATP hydrolysis was initiated by the addition of 2 μM RecA and after an additional 16 min incubation, RecX protein was added (RecX concentrations are indicated in the figure legends). NADH depletion was measured every 2 min, at 340 nm, in a Spectramax M5 microplate spectrophotometer equipped with Softmax PRO software (Molecular Devices), using flat-bottom UV-transparent 96-well microplates (Costar). Reaction volumes were 200 μl each and measurements were taken at 37°C. Absorption data were translated into NADH concentration using a standard NADH concentration curve.

Strand-exchange assay

Strand-exchange assays were performed as described (Drees *et al*, 2004a). All incubations were at 37°C. RecA (6.3 μM) was pre-incubated for 10 min with 20 μM (nucleotide concentration) ϕX174 circular ssDNA (New England Biolabs) in the SE buffer, in the presence of 1 mM DTT, an ATP-regenerating system consisting of 3 mM PEP and 10 U/ml pyruvate kinase (Sigma). SSB (2 μM) and ATP (3 mM) were added and incubation was continued for six more minutes. RecX was then added to the reactions at the concentrations indicated in the figure. After an additional 6 min incubation, the strand-exchange reaction was initiated by the addition of 20 μM AatII-linearised ϕX174 circular dsDNA. The reactions were terminated after 45 min by the addition of 1 × TAE, 5% glycerol, 0.2% SDS, 4 mM EDTA and 0.05% bromophenol blue (final concentrations). The samples were analysed by 0.8% agarose/TBE gel electrophoresis containing 0.5 μg/ml ethidium bromide. The gels were stained with GelRed (Biotium) following the manufacturer's protocol, exposed to UV trans-illuminator and images were captured with a digital CCD camera.

SPR

RecA–ssDNA interactions were analysed with a BIAcore 2000 SPR biosensor (BIAcore; GE Healthcare). SPR experiments were carried out at a flow rate of 10 μl/min in the SE buffer containing 0.008% P20. An SA-coated sensor chip (GE Healthcare) was derivatised with three 2-min injections of 1 nM 5′-biotinylated, polydT 60-mer (Sigma), up to a level of approximately 135 RU. RecA at a concentration of 4 μM was injected onto the sensor chip for 1 min, followed by a 1.5-min injection of RecX. In all experiments, the control sensorgram of the reference flow channel (channel 1), which did not have bound DNA, was subtracted from the experimental sensorgram (channel 2). In separate control experiments performed under identical experimental conditions, we determined that RecX does not bind to the polydT 60-mer at the concentrations used in the assay (data not shown). The oligo-bound SA sensor chip was regenerated between experiments with a 1-min injection (10 μl/min) of 50 mM NaOH and 1 M NaCl. Negligible loss of DNA was detected after the regeneration step.

Supplementary data

Supplementary data are available at *The EMBO Journal* Online (http://www.embojournal.org).

Acknowledgements

We are grateful to Ed Egelman for providing the EM reconstruction of the RecA–RecX–DNA filament and for help in docking the RecX structure. We thank Scott Singleton for the gift of the pTXB-recA3 vector, Martin Moncrieff for help with analytical ultracentrifugation and Vincent Millischer for assistance in preparing the figures. This study was supported by a Wellcome Trust senior research fellowship in basic biomedical sciences to LP. SR was supported by a PhD studentship of the University of Turin, Italy. JDM was supported by the Wellcome Trust. NF was supported by a Biotechnology and Biological Sciences Research Council PhD studentship.

References

Arenson TA, Tsodikov OV, Cox MM (1999) Quantitative analysis of the kinetics of end-dependent disassembly of RecA filaments from ssDNA. *J Mol Biol* **288:** 391–401

Bailone A, Backman A, Sommer S, Celerier J, Bagdasarian MM, Bagdasarian M, Devoret R (1988) PsiB polypeptide prevents activation of RecA protein in *Escherichia coli*. *Mol Gen Genet* **214:** 389–395

Baker NA, Sept D, Joseph S, Holst MJ, McCammon JA (2001) Electrostatics of nanosystems: application to microtubules and the ribosome. *Proc Natl Acad Sci USA* **98:** 10037–10041

Bianco PR, Tracy RB, Kowalczykowski SC (1998) DNA strand exchange proteins: a biochemical and physical comparison. *Front Biosci* **3:** D570–D603

Bork JM, Cox MM, Inman RB (2001a) RecA protein filaments disassemble in the 5′–3′ direction on single-stranded DNA. *J Biol Chem* **276:** 45740–45743

Bork JM, Cox MM, Inman RB (2001b) The RecOR proteins modulate RecA protein function at 5′ ends of single-stranded DNA. *EMBO J* **20:** 7313–7322

Brendel V, Brocchieri L, Sandler SJ, Clark AJ, Karlin S (1997) Evolutionary comparisons of RecA-like proteins across all major kingdoms of living organisms. *J Mol Evol* **44:** 528–541

Chabbert M, Cazenave C, Helene C (1987) Kinetic studies of recA protein binding to a fluorescent single-stranded polynucleotide. *Biochemistry* **26:** 2218–2225

Chen Z, Yang H, Pavletich NP (2008) Mechanism of homologous recombination from the RecA–ssDNA/dsDNA structures. *Nature* **453:** 489–494

Cisse I, Okumus B, Joo C, Ha T (2007) Single-molecule chemistry and biology special feature: fueling protein DNA interactions inside porous nanocontainers. *Proc Natl Acad Sci USA* **104:** 12646–12650

Cox MM (2007a) Motoring along with the bacterial RecA protein. *Nat Rev Mol Cell Biol* **8:** 127–138

Cox MM (2007b) Regulation of bacterial RecA protein function. *Crit Rev Biochem Mol Biol* **42:** 41–63

Drees JC, Lusetti SL, Chitteni-Pattu S, Inman RB, Cox MM (2004a) A RecA filament capping mechanism for RecX protein. *Mol Cell* **15:** 789–798

Drees JC, Lusetti SL, Cox MM (2004b) Inhibition of RecA protein by the *Escherichia coli* RecX protein: modulation by the RecA C terminus and filament functional state. *J Biol Chem* **279:** 52991–52997

Emsley P, Cowtan K (2004) Coot: model-building tools for molecular graphics. *Acta Crystallogr D Biol Crystallogr* **60:** 2126–2132

Furnham N, Dore AS, Chirgadze DY, de Bakker PIW, DePristo MA, Blundell TL (2006) Knowledge-based real-space explorations for low-resolution structure determination. *Structure* **14:** 1313–1320

Galletto R, Amitani I, Baskin RJ, Kowalczykowski SC (2006) Direct observation of individual RecA filaments assembling on single DNA molecules. *Nature* **443:** 875–878

Gallivan JP, Dougherty DA (1999) Cation–pi interactions in structural biology. *Proc Natl Acad Sci USA* **96:** 9459–9464

Galvao CW, Pedrosa FO, Souza EM, Yates MG, Chubatsu LS, Steffens MBR (2004) Expression, purification, and DNA-binding activity of the *Herbaspirillum seropedicae* RecX protein. *Protein Expr Purif* **35:** 298–303

Hobbs MD, Sakai A, Cox MM (2007) SSB protein limits RecOR binding onto single-stranded DNA. *J Biol Chem* **282:** 11058–11067

Joo C, McKinney SA, Nakamura M, Rasnik I, Myong S, Ha T (2006) Real-time observation of reca filament dynamics with single monomer resolution. *Cell* **126:** 515–527

Kiianitsa K, Solinger JA, Heyer WD (2003) NADH-coupled microplate photometric assay for kinetic studies of ATP-hydrolyzing enzymes with low and high specific activities. *Anal Biochem* **321:** 266–271

Kowalczykowski SC (2000) Initiation of genetic recombination and recombination-dependent replication. *Trends Biochem Sci* **25:** 156–165

Kowalczykowski SC, Krupp RA (1987) Effects of *Escherichia coli* SSB protein on the single-stranded DNA-dependent ATPase activity of *Escherichia coli* RecA protein. Evidence that SSB protein facilitates the binding of RecA protein to regions of secondary structure within single-stranded DNA. *J Mol Biol* **193:** 97–113

La Fortelle ED, Bricogne G (1997) Maximum-likelihood heavy-atom parameter refinement for multiple isomorphous replacement and multiwavelength anomalous diffraction methods. *Methods Enzymol* **276:** 472–494

Landau M, Mayrose I, Rosenberg Y, Glaser F, Martz E, Pupko T, Ben-Tal N (2005) ConSurf 2005: the projection of evolutionary conservation scores of residues on protein structures. *Nucleic Acids Res* **33:** W299–W302

Lavery PE, Kowalczykowski SC (1990) Properties of recA441 protein-catalyzed DNA strand exchange can be attributed to an enhanced ability to compete with SSB protein. *J Biol Chem* **265:** 4004–4010

Lindsley JE, Cox MM (1990) Assembly and disassembly of RecA protein filaments occur at opposite filament ends. Relationship to DNA strand exchange. *J Biol Chem* **265:** 9043–9054

Lusetti SL, Cox MM (2002) The bacterial RecA protein and the recombinational DNA repair of stalled replication forks. *Annu Rev Biochem* **71:** 71–100

Lusetti SL, Hobbs MD, Stohl EA, Chitteni-Pattu S, Inman RB, Seifert HS, Cox MM (2006) The RecF protein antagonizes RecX function via direct interaction. *Mol Cell* **21:** 41–50

Lusetti SL, Voloshin ON, Inman RB, Camerini-Otero RD, Cox MM (2004) The DinI protein stabilizes RecA protein filaments. *J Biol Chem* **279:** 30037–30046

McCoy AJ, Grosse-Kunstleve RW, Adams PD, Winn MD, Storoni LC, Read RJ (2007) Phaser crystallographic software. *J Appl Crystallogr* **40:** 658–674

McGhee JD, Von Hippel PH (1974) Theoretical aspects of DNA–protein interactions: co-operative and non-co-operative binding of large ligands to a one-dimensional lattice. *J Mol Biol* **86:** 469–489

Mendonca VM, Kaiser-Rogers K, Matson SW (1993) Double helicase II (uvrD)–helicase IV (helD) deletion mutants are defective in the recombination pathways of *Escherichia coli*. *J Bacteriol* **175:** 4641–4651

Moore T, McGlynn P, Ngo HP, Sharples GJ, Lloyd RG (2003) The RdgC protein of *Escherichia coli* binds DNA and counters a toxic effect of RecFOR in strains lacking the replication restart protein PriA. *EMBO J* **22:** 735–745

Morel P, Hejna JA, Ehrlich SD, Cassuto E (1993) Antipairing and strand transferase activities of *E. coli* helicase II (UvrD). *Nucleic Acids Res* **21:** 3205–3209

Morimatsu K, Kowalczykowski SC (2003) RecFOR proteins load RecA protein onto gapped DNA to accelerate DNA strand exchange: a universal step of recombinational repair. *Mol Cell* **11:** 1337–1347

Morris RJ, Perrakis A, Lamzin VS (2003) ARP/wARP and automatic interpretation of protein electron density maps. In: *Macromolecular Crystallography, Part D*, Carter CWJ, Sweet RM (eds), Vol. 374, pp 229–244. Academic Press

Murshudov GN, Vagin AA, Dodson EJ (1997) Refinement of macromolecular structures by the maximum-likelihood method. *Acta Crystallogr D Biol Crystallogr* **53:** 240–255

Pages V, Koffel-Schwartz N, Fuchs RPP (2003) recX, a new SOS gene that is co-transcribed with the recA gene in *Escherichia coli*. *DNA Repair* **2:** 273–284

Papavinasasundaram KG, Movahedzadeh F, Keer JT, Stoker NG, Colston MJ, Davis EO (1997) Mycobacterial recA is cotranscribed with a potential regulatory gene called recX. *Mol Microbiol* **24:** 141–153

Roca AI, Cox MM (1997) RecA protein: structure, function, and role in recombinational DNA repair. *Prog Nucleic Acid Res Mol Biol* **56:** 129–223

Sano Y (1993) Role of the recA-related gene adjacent to the recA gene in *Pseudomonas aeruginosa*. *J Bacteriol* **175:** 2451–2454

Schlacher K, Pham P, Cox MM, Goodman MF (2006) Roles of DNA polymerase V and RecA protein in SOS damage-induced mutation. *Chem Rev* **106:** 406–419

Schwarz G, Watanabe F (1983) Thermodynamics and kinetics of co-operative protein–nucleic acid binding. I. General aspects of analysis of data. *J Mol Biol* **163:** 467–484

Shan Q, Bork JM, Webb BL, Inman RB, Cox MM (1997) RecA protein filaments: end-dependent dissociation from ssDNA and stabilization by RecO and RecR proteins. *J Mol Biol* **265:** 519–540

Singleton SF, Simonette RA, Sharma NC, Roca AI (2002) Intein-mediated affinity-fusion purification of the *Escherichia coli* RecA protein. *Protein Expr Purif* **26:** 476–488

Stohl EA, Brockman JP, Burkle KL, Morimatsu K, Kowalczykowski SC, Seifert HS (2003) *Escherichia coli* RecX inhibits RecA recombinase and coprotease activities *in vitro* and *in vivo*. *J Biol Chem* **278:** 2278–2285

Sukchawalit R, Vattanaviboon P, Utamapongchai S, Vaughn G, Mongkolsuk S (2001) Characterization of *Xanthomonas oryzae* pv. *oryzae* recX, a gene that is required for high-level expression of recA. *FEMS Microbiol Lett* **205:** 83–89

Sung P, Klein H (2006) Mechanism of homologous recombination: mediators and helicases take on regulatory functions. *Nat Rev Mol Cell Biol* **7:** 739–750

Umezu K, Chi N, Kolodner RD (1993) Biochemical Interaction of the *Escherichia coli* RecF, RecO, and RecR proteins with RecA protein and single-stranded DNA binding protein. *Proc Natl Acad Sci USA* **90:** 3875–3879

Umezu K, Kolodner RD (1994) Protein interactions in genetic recombination in *Escherichia coli*. Interactions involving RecO and RecR overcome the inhibition of RecA by single-stranded DNA-binding protein. *J Biol Chem* **269:** 30005–30013

van Gent DC, Hoeijmakers JHJ, Kanaar R (2001) Chromosomal stability and the DNA double-stranded break connection. *Nat Rev Genet* **2:** 196–206

VanLoock MS, Yu X, Yang S, Galkin VE, Huang H, Rajan SS, Anderson WF, Stohl EA, Seifert HS, Egelman EH (2003) Complexes of RecA with LexA and RecX differentiate between active and inactive RecA nucleoprotein filaments. *J Mol Biol* **333:** 345–354

Veaute X, Delmas S, Selva M, Jeusset J, Le Cam E, Matic I, Fabre F, Petit MA (2005) UvrD helicase, unlike Rep helicase, dismantles RecA nucleoprotein filaments in *Escherichia coli*. *EMBO J* **24:** 180–189

Venkatesh R, Ganesh N, Guhan N, Reddy MS, Chandrasekhar T, Muniyappa K (2002) RecX protein abrogates ATP hydrolysis and strand exchange promoted by RecA: Insights into negative regulation of homologous recombination. *Proc Natl Acad Sci USA* **99:** 12091–12096

Vierling S, Weber T, Wohlleben W, Muth G (2000) Transcriptional and mutational analyses of the *Streptomyces lividans* recX gene and its interference with RecA activity. *J Bacteriol* **182:** 4005–4011

Webb BL, Cox MM, Inman RB (1997) Recombinational DNA repair: the RecF and RecR proteins limit the extension of RecA filaments beyond single-strand DNA gaps. *Cell* **91:** 347–356

Weeks CM, Miller R (1999) The design and implementation of *SnB* version 2.0. *J Appl Cryst* **32:** 120–124

West SC (2003) Molecular views of recombination proteins and their control. *Nat Rev Mol Cell Biol* **4:** 435–445